Pergamon

Journal of Structural Geology, Vol. 18, No. 8, pp. 1017 to 1029, 1996
Copyright © 1996 Elsevier Science Ltd
Printed in Great Britain. All rights reserved
PII: S0191-8141(96)00036-3
0191-8141/96 $15.00 + 0.00

Structural analysis and fault segment boundary identification along the Hurricane fault in southwestern Utah

MEG E. STEWART* and WANDA J. TAYLOR

Department of Geoscience, University of Nevada, Las Vegas, NV 89154-4010, U.S.A.

(*Received* 13 *February* 1995; *accepted in revised form* 11 *April* 1996)

Abstract—Long normal fault zones are common in extending regions and can be divided into segments with different geometries and faulting histories based on surface observations. The boundaries between fault segments are important because they may be the sites of significant strain, may impede rupture propagation, and may greatly influence the locations of earthquakes. Because large geometric bends exist at some fault segment boundaries throughout the history of the boundary, we suggest that such bends can last throughout much of the life of the fault.

We use fault segmentation concepts to define a segment boundary and parts of two fault segments along the active Hurricane normal fault, southwestern Utah, U.S.A. We use fault geometry, slip direction, shortening structures in the hanging wall and footwall, and fault scarp morphology to identify the fault segments and segment boundary. The fault strikes N13°W south of the boundary and N21°E north of the boundary. Stratigraphic separation of geochemically identical Quaternary basalt in the footwall and the hanging wall suggests that the slip vector of Quaternary displacement trends between N70°W and S18°W, and slickenlines, earthquake rakes, and dip analysis on syndeformational basalt further constrains the slip direction to N75–85°W. Relative motion on the northern segment, termed here the Ash Creek segment, is purely dip-slip, and on the southern (Anderson Junction) segment is dominantly dip-slip with a small dextral slip component. Fault scarps along the Ash Creek segment compared with offset gravels lacking scarps along the Anderson Junction segment suggest that the two segments have different Late Quaternary faulting histories, which is indicative of discrete fault segments. The Ash Creek segment is about 24 km long and the Anderson Junction segment is 19–45 km long, although the non-adjacent segment terminations remain poorly defined. The segment boundary zone consists of: (1) a small-scale hanging wall anticline that trends roughly normal to the fault; (2) a small-offset footwall thrust fault; and (3) space-filling imbricate normal faults in the hanging wall. Secondary structures suggest the segment boundary is a non-conservative boundary. Copyright © 1996 Elsevier Science Ltd

INTRODUCTION

Long normal fault zones are typical of many extending regions, including the seismically active parts of the Basin and Range province and the transition zone between the Basin and Range province and the Colorado Plateau. These long faults can be divided into segments that have different geometries, faulting histories and seismicity histories (e.g. Schwartz & Coppersmith 1984, Bruhn *et al.* 1987, 1990, Susong *et al.* 1990, dePolo *et al.* 1991). Therefore, it is possible to define fault segments and segment boundaries based on surface observations of fault geometry, scarps and kinematic indicators. Fault segment boundaries are significant because prior studies of normal fault segmentation concluded that segment boundaries may be the sites of significant strain, may impede rupture propagation, and may greatly influence the locations of earthquakes (e.g. Schwartz & Coppersmith 1984, King 1986, Bruhn *et al.* 1987, 1990, Susong *et al.* 1990, dePolo *et al.* 1991, Machette *et al.* 1991, Zhang *et al.* 1991, Janecke 1993, Evans & Langrock 1994). Identification of discrete fault segments and boundaries is critical for seismic risk analysis because fault segment length provides an estimate of the maximum length that a fault is likely to rupture.

Another important aspect of fault segment boundaries is that they form early in the life or history of a fault. Fault growth models suggest segment boundaries and the large geometrical fault bends typically associated with them form as (1) two (or more) propagating fractures approach each other and then link or (2) pre-existing fractures, such as joints, are linked by tensile fractures (Cowie & Scholz 1992a,b). We suggest that the major geometric bends formed at the segment boundaries can last throughout much of the life of the fault. Geometrical bends at segment boundaries can be shown to be a major geometric component of a fault even once the fault segments are fully linked.

We use new data from along the Hurricane fault in southwestern Utah to define a segment boundary and parts of the two enclosing segments. These data suggest that the fault segment boundary and the associated bend persists throughout much of the life of the fault and allows future seismic risk assessment along this fault. The Hurricane fault is a major, active, high-angle, west-dipping normal fault that lies along the Colorado Plateau–Basin and Range province transition zone (Fig. 1). We analyze in detail part of the Hurricane fault to define a segment boundary in order to gain clearer knowledge of the relationship between fault segmentation and the life span of fault bends as well as seismicity in this seismically active region (Smith & Sbar 1974, Arabasz & Smith 1981, Anderson & Christenson 1989, Arabasz *et al.* 1992a,b, Christenson & Nava 1992).

Fault segments have not been previously identified along the Hurricane fault in Utah. The present work employs a larger map scale (1:12,000 scale in Schramm 1994) which furnished detail for the analysis of structures found in the excellent exposures of both the hanging wall

* Now at: Dames and Moore, One Blue Hill Plaza, Pearl River, NY 10965-1668, U.S.A.

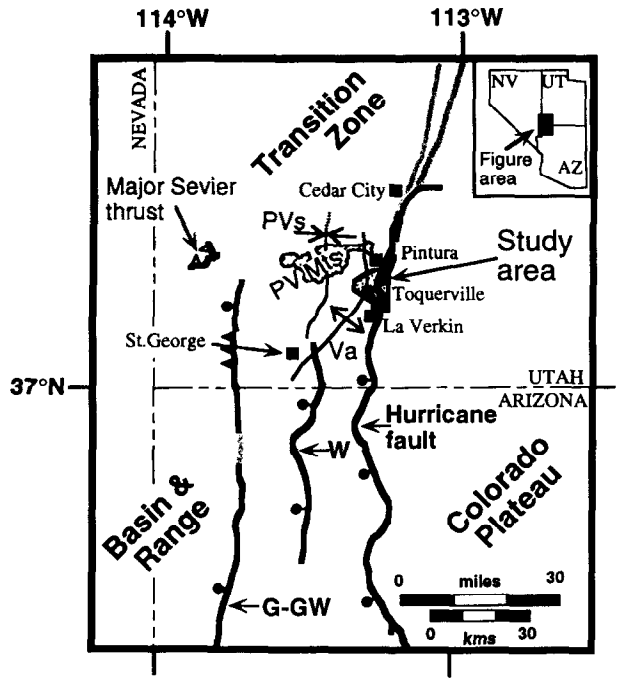

Fig. 1. Locations of major faults in southwestern Utah and northwestern Arizona (bar and ball on downthrown side, stippled where the fault is concealed; teeth on upper plate.): the Hurricane fault, W = Washington fault, and G–GW = Gunlock–Grand Wash fault. The Hurricane fault appears to splay to north where it is concealed. The major folds are: PVs = Pine Valley syncline; Va = Virgin anticline. Major thrust is the Sevier-age Square Top Mountain thrust. Area outlined and stippled is the study area and is shown in greater detail in Fig. 2. Structural data compiled from Hintze (1975) and Reynolds (1988).

and footwall of the Hurricane fault. This study focuses on: (1) the kinematics of two segments of the fault, the boundary between them, including total amount of stratigraphic separation, sense of motion, and direction of motion; (2) the amounts of stratigraphic separation observed in the Quaternary igneous and sedimentary units; (3) the structural effects of a fault segment boundary on the hanging wall and footwall blocks; and (4) the relationship between the Hurricane fault and the nearby regional-scale folds.

GEOLOGIC BACKGROUND

The Hurricane fault study area is located approximately 30 km northeast of St. George, Utah (Fig. 1). The 92 km^2 mapped area straddles the Hurricane fault. To the east are the relatively flat-lying strata of the Colorado Plateau. To the west are the Pine Valley Mountains, predominantly composed of a large Cenozoic laccolith, and the deep basins and high ranges typical of the Basin and Range province (Huntington & Goldthwait 1904, Dobbin 1939, Gardner 1941, Cook 1957, Averitt 1962, Lovejoy 1964, Hamblin 1965, 1970, Kurie 1966, Watson 1968, Anderson & Mehnert 1979, Schramm 1994).

The study area contains Paleozoic and Mesozoic rocks that predate all exposed deformation in the region (Armstrong 1968). During the Cretaceous, thrust faults of the Sevier orogenic belt cut the area west and northwest of the Hurricane fault and Pine Valley Mountains, moderately folding and warping older rocks (Fig. 1) (Armstrong 1968, Cowan & Bruhn 1992).

During the early and middle Tertiary the study area underwent a period of tectonic quiescence (Cook 1957). Major regional magmatism occurred in the area during the Oligocene and Miocene, with volcanism beginning at about 33 Ma just north of the Pine Valley Mountains and migrating southward in time (e.g. Rowley *et al.* 1979, Best & Grant 1987, Best *et al.* 1989). Between $\approx$20 and 22 Ma the Pine Valley laccolith and other intrusions were emplaced (Armstrong 1963, Nelson *et al.* 1992). Extension began in the Oligocene north of the Pine Valley Mountains and in the Miocene in the vicinity of the Pine Valley Mountains (Gardner 1941, Cook 1952, 1957, Mackin 1960, Taylor & Bartley 1992, Axen *et al.* 1993). Extension continued from the Miocene into the Quaternary in the vicinity of the Pine Valley Mountains and the Hurricane fault.

The Hurricane fault is 250 km long and the age of first motion on the fault is unknown. Based on stratigraphic and structural relationships some workers suggest an initiation age of Miocene (Gardner 1941, Averitt 1964, Hamblin 1970), or contemporaneously with laccolith emplacement (Cook 1957). Others suggest Pliocene or Pleistocene initial motion for some sections of the fault (Anderson & Mehnert 1979, Anderson & Christenson 1989). Anderson & Mehnert (1979) assert that only up to 850 m of total displacement occurred along the fault based on the structural level of the top of the Navajo Sandstone. Near Toquerville, Utah, we document 450 m of stratigraphic separation of Quaternary basalt and a total stratigraphic separation of up to 2520 m. Because the basalt is offset less than older units, motion on the Hurricane fault initiated prior to basaltic volcanism and is likely to have begun as early as Late Miocene or Early Pliocene. However, the basalt in this area has not been dated, so rates of slip cannot be defined.

Although the age of onset of motion along the Hurricane fault is unknown, the fault has been active in the Quaternary. A recent magnitude 5.8 earthquake that occurred on or near the Hurricane fault suggests the fault may be active (Arabasz *et al.* 1992a,b, Pechmann *et al.* 1992), and our new mapping of three fault scarps provides evidence of young surface offset.

The Hurricane fault has been called a normal dip-slip fault (Huntington & Goldthwait 1904, Gardner 1941, Cook 1957, Averitt 1962, Hamblin 1965, 1970, Kurie 1966), a reverse fault (Lovejoy 1964), and Moody & Hill (1956) proposed that the Hurricane fault had a significant left-slip component along it. The theory that the fault is a left-slip fault has again been recently suggested (Anderson & Barnhard 1993).

BASALT CORRELATION

For analysis of structural relationships along the Hurricane fault, the Quaternary basalt that is offset by

the fault is described in detail. Basalt crops out in the hanging wall and footwall of the Hurricane fault and consists of six individual pahoehoe and aa flows each from 3 to 9 m thick. The flows appear to have been extruded in a relatively brief time span because no evidence of soil formation between flows was observed. The rocks have not been dated, but similar basalt in the vicinity was dated by the K/Ar method and falls between 0.3 and 1.1 Ma (Best *et al.* 1980) and an $^{40}Ar/^{39}Ar$ isochron date yielded 353 ± 45 ka for geochemically similar basalt (Sanchez 1995).

Basalt from three locations was studied in thin section for the purpose of correlating flows across the Hurricane fault. The upper and lower basalt flows collected both from the hanging wall and the footwall do not uniquely correlate. All sampled locations have very similar mineral assemblages.

We used whole-rock trace element X-ray fluorescence (XRF) spectrometry to fingerprint basalt samples collected from two locations in the hanging wall of the Hurricane fault and one location from the footwall to establish a chemical stratigraphy. Samples were collected from corresponding stratigraphic intervals at: AC (Ash Creek), T (Toquerville), and P (Pintura) (Fig. 2). Thirteen basalt samples were analyzed to determine whether lava flows in the footwall of the Hurricane fault were the same as the flow rocks in the hanging wall (Table 1). If these are the same flows, then a slip vector and amount of Quaternary offset can be measured because the flows are essentially wide but linear features that form piercing points. The piercing point formed by the basalt is confirmed because the lower units exposed in the footwall occupy a paleochannel. Flow structures such as pipe amygdules occur in the lower basalt in the footwall (site T) corroborating that the paleotopography was the observable paleovalley during basalt extrusion. Samples were collected from the middle of this channel for the T sample to minimize effects of contamination. Detailed methods are listed in the Appendix.

The trace element data (Table 1) show striking positive correlations between flows at different sections (Fig. 3). The lowest flows at sites AC (in the hanging wall) and T (in the footwall) exhibit clear groupings in trace element plots suggesting that they are genetically related. The lowest unit at site P (also in the hanging wall) is not related to the lowest unit at the two southern sampling sites (AC and T). Flows 2 to 5 at all three sampling locations appear to correlate. This agrees with mineral modes determined in hand specimen and thin section.

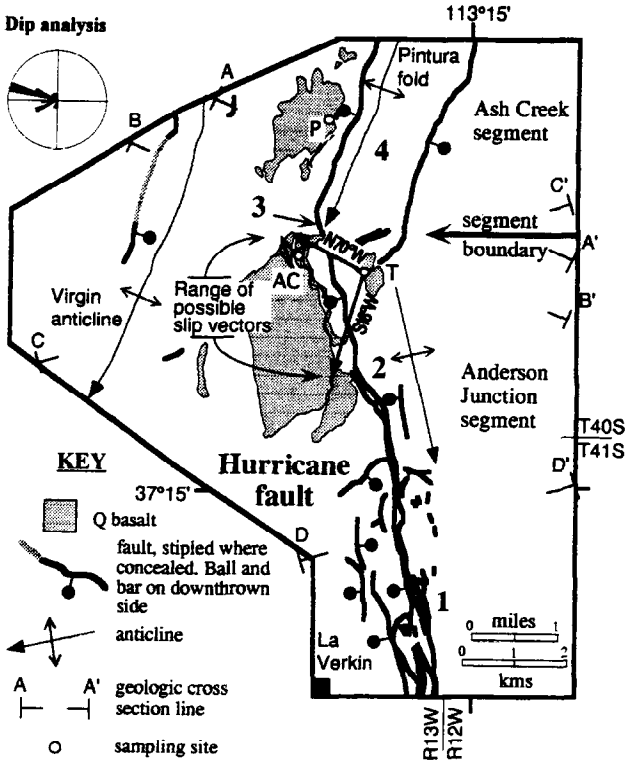

Fig. 2. Simplified structure map of the Hurricane fault study area in Utah. Cenozoic basalt fields are stippled. Fault sections are labeled with 1, 2, 3 and 4. Cross-sections A–A′ through D–D′ are shown constructed in Fig. 4. Circles indicate where basalt sections were sampled: T = Toquerville, AC = Ash Creek, and P = Pintura. The range of possible slip vectors (between 73°, N70°W and 75°, S18°W) was determined by geochemically correlating basalt at T with basalt at AC using the X-ray fluorescence method and assuming that the basalt field that AC was collected from is homogeneous. The stereoplot in the upper left is a dip analysis of the bedding attitudes of basalt in the hanging wall of the Hurricane fault (after Scott *et al.*, 1994). The computed mean vector is N84°W and the median is N75°W. The data (n = 20) were plotted on an equal area net using R. W. Allmendinger's *Stereonet*. Two fault segments, the Ash Creek segment and the Anderson Junction segment, and a fault segment boundary are shown.

STRUCTURAL GEOLOGY

Description of the Hurricane fault zone

Our observations of the structural geology in the map area will be discussed first and our interpretations of these data will follow. The Hurricane fault was found to be: (1) a dominantly dip-slip fault; (2) a fault with a large stratigraphic separation; (3) a segmented fault; (4) locally a fault zone or locally a single fault strand; (5) an active fault; and (6) a high-angle extensional fault, unrelated to pre-existing thrust faults and folds. We also observed shortening structures close to the fault trace.

Slip direction along the Hurricane fault zone

A variety of types of data are used to constrain the slip direction along the Hurricane fault. For example, a range of possible slip vectors is determined from a very broad piercing point formed by a chemically similar basalt section in the hanging wall and a mostly channel confined basalt section in the footwall. The range is then restricted by slickenlines, the rake of an earthquake focal mechanism and secondary structures. This combination of data suggests the fault has had dominantly dip-slip motion along it in the Quaternary. No evidence was found to support a dominantly strike-slip sense of motion along the Hurricane fault in this location during the Quaternary. The fault was mapped for 13 km along strike and an emphasis is placed on kinematics and structures at fault

Table 1. Major and trace elements determined by the XRF technique for whole rock basalt samples. Sample number (P, AC, T) corresponds to locations shown in Fig. 2. Analytical precision and accuracy in % are compared with the standard BIR-1 (* indicates comparison with GSP-1) for major elements and BHVO-1 for trace elements. All are USGS standards

sample #	P-0-93	P-1-93	P-2-93	P-3-93	P-4-93	AC-1-93	AC-2-93	AC-3-93	T-1-93	T-2-93	T-3-93	T-4-93	T-5-93	BIR-1 Precision	BIR-1 Accuracy
Wt %															
SiO_2	49.5	51.8	51.2	51.7	51.7	50.2	50.4	50.4	49.5	51.3	50.5	48.9	48.9	0.32	0.06
TiO_2	1.6	1.5	1.5	1.5	1.6	1.9	1.9	1.6	2.0	1.6	1.7	1.8	1.6	0.84	1.04
Al_2O_3	16.6	16.2	15.2	16.0	16.2	16.1	15.8	16.1	15.8	16.2	16.1	15.8	16.3	0.54	2.40
Fe_2O_3	10.7	9.9	9.9	9.8	10.4	10.0	12.0	11.3	10.6	11.2	11.3	12.6	12.0	0.47	0.26
MnO	0.1	0.1	0.1	0.1	0.1	0.2	0.2	0.2	0.2	0.2	0.2	0.2	0.2	2.91	3.89
MgO	6.2	5.5	5.6	5.5	6.5	8.2	6.3	6.7	8.0	6.6	6.6	7.4	7.4	*1.82	*2.99
CaO	10.4	9.1	9.3	9.3	9.1	8.1	9.7	9.5	8.4	9.4	9.7	10.1	10.1	2.86	2.12
Na_2O	2.7	2.8	2.7	2.8	3.4	3.8	3.4	3.3	3.5	3.4	3.4	3.2	3.1	1.36	1.90
K_2O	0.7	1.0	0.9	1.1	1.1	1.4	0.9	0.9	1.4	1.0	0.9	0.7	0.6	0.22	0.59
P_2O_5	0.3	0.3	0.3	0.3	0.3	0.5	0.3	0.3	0.5	0.3	0.3	0.3	0.3	*2.50	*15.18
Total wt %	98.6	98.2	96.8	98.1	100.3	100.3	100.7	100.3	99.9	101.3	100.6	100.8	100.5		
ppm														BHVO-1 Precision	BHVO-1 Accuracy
Rb	10.0	18.0	11.9	19.8	20.3	16.9	18.6	18.5	17.3	18.8	17.3	13.3	8.7	2.04	2.42
Ba	395	644	758	635	745	519	444	551	538	546	540	427	384	7.34	78.96
Nb	9.9	10.1	10.9	12.3	10.3	23.6	11.9	10.3	24.3	9.4	11.6	10.0	9.0	8.22	19.62
Sr	436	547	545	534	539	703	453	505	715	515	508	473	439	0.66	3.96
Zr	162	206	210	212	215	263	188	187	272	193	192	177	162	1.82	1.71
Y	21.9	21.9	22.4	22.9	23.1	22.2	22.8	22.6	21.8	22.4	21.8	22.1	21.1	1.53	21.27
Cr	214	227	334	370	259	93	148	185	217	295	193	208	146	5.65	5.33
Ni	76	72	73	70	63	162	55	64	175	56	70	71	62	31.82	5.19

segment boundaries, so processes discussed here may not be applicable for the entire fault length of over 250 km.

The geochemical correlation of Quaternary basalt flows provides strong evidence that motion on the Hurricane fault after basalt extrusion has been nearly perfect normal dip-slip. The fact that all the flows at sites T and AC are geochemically identical (Fig. 3), indicate displacement nearly parallel to the median fault dip direction, and the hanging wall site, AC, was down-dropped relative to site footwall site T (Fig. 2). The flows at site AC and T were once adjacent to each other (or nearly so) and now make up a large piercing point for motion on the Hurricane fault in the Quaternary. Basalt samples were not analyzed to the south of AC, but if it is assumed that the basalt field from which the AC samples were collected from is homogeneous, then the trend and plunge of the slip vector since basalt emplacement, could be between 73°, N70°W and 75°, S18°W.

Normal dip-slip displacement is corroborated by slickenside lineations measured at four locations exposed on the Hurricane fault. The rakes of these four lines of direction of last motion, range from 74° to vertical. In addition, Kurie (1966) reported vertical slickenlines on the Hurricane fault.

Further evidence that the Hurricane fault is dominantly a dip-slip fault is the rake of the St. George, Utah, September 2, 1992 (M_W = 5.8) earthquake. The P-wave first motion focal mechanisms for the earthquake indicate an average rake of $-89° \pm 14°$ (Lay *et al.* 1994) and this earthquake may have occurred on a southern segment of the Hurricane fault (Arabasz *et al.* 1992b). Sparse seismic stations in the area render determination of which fault this earthquake occurred on equivocal. The earthquake occurred at 15 ± 5 km depth and the surface projection of the west-dipping nodal plane lies very close to the surface trace of the Hurricane fault. This suggests, but is not conclusive evidence, that the main shock resulted from buried slip on the Hurricane fault (Pechmann *et al.* 1992).

The bedding attitudes of syndeformational basalt should generally reflect the shape of the fault (Walker 1986, Scott *et al.* 1994). Theoretically, if the sense of motion on a fault is purely dip-slip and the fault dip direction is relatively constant with depth, then the hanging wall dip direction will be exactly opposite to the dip of the section of the fault along which the block containing the syndeformational deposits slipped. Twenty data points were used to determine the median dip direction of the hanging wall basalt. Dip analysis is not intended here or used here as a stand-alone technique. Fault motion direction analysis using bedding attitudes collected from the basalt in the hanging wall of the fault indicates that a large number of basalt dip direction data plot between N70°W and N80°W (Fig. 2) (cf. Scott *et al.* 1994). The median direction of motion of the hanging wall relative to the footwall is N75°W and the mean direction of motion is N84°W. In the basalt fields where dip data were collected, the fault strikes N13°W (near '3' on Fig. 2) and N21°E (near '4'). Therefore, along these sections of the fault a median direction of motion, N75°W, corroborates a generally normal sense of motion along the Hurricane fault in the Quaternary and that the hanging wall block dip direction may have been controlled by the intersection of the fault sections.

Stratigraphic separation

The magnitude of stratigraphic separation of the Quaternary basalt is 450 m (Fig. 4, cross-section C–C').

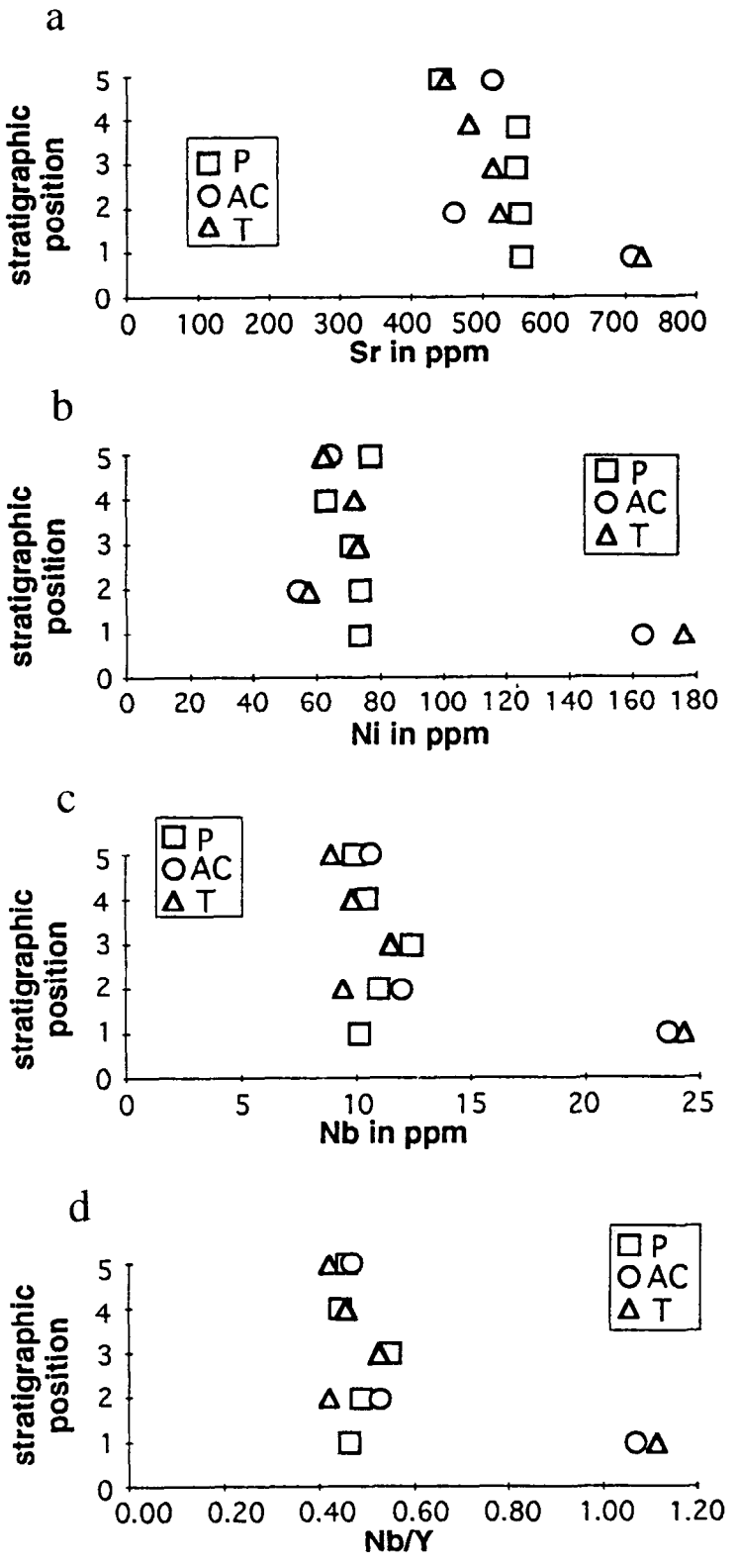

Fig. 3. (a) Plot of Sr in ppm versus stratigraphic position for basalt flows collected at sites P, AC, and T which are labeled on Fig. 2. (b) Plot for the element Ni. The correlation of Ni is indicative of the presence of mafic minerals in constant proportions in flows two and above (stratigraphic positions 2 to 5). (c) Plot of the incompatible element Nb in ppm versus stratigraphic position. (d) is a ratio of incompatible elements Nb and Y versus stratigraphic position for basalt flows at sites P, AC, and T. The plot of Nb/Y, both highly incompatible elements in basalt, shows conclusively that flows two and above are related at all three sampling sites and the lowest flow at the T and AC locations is a distinct and separate unit.

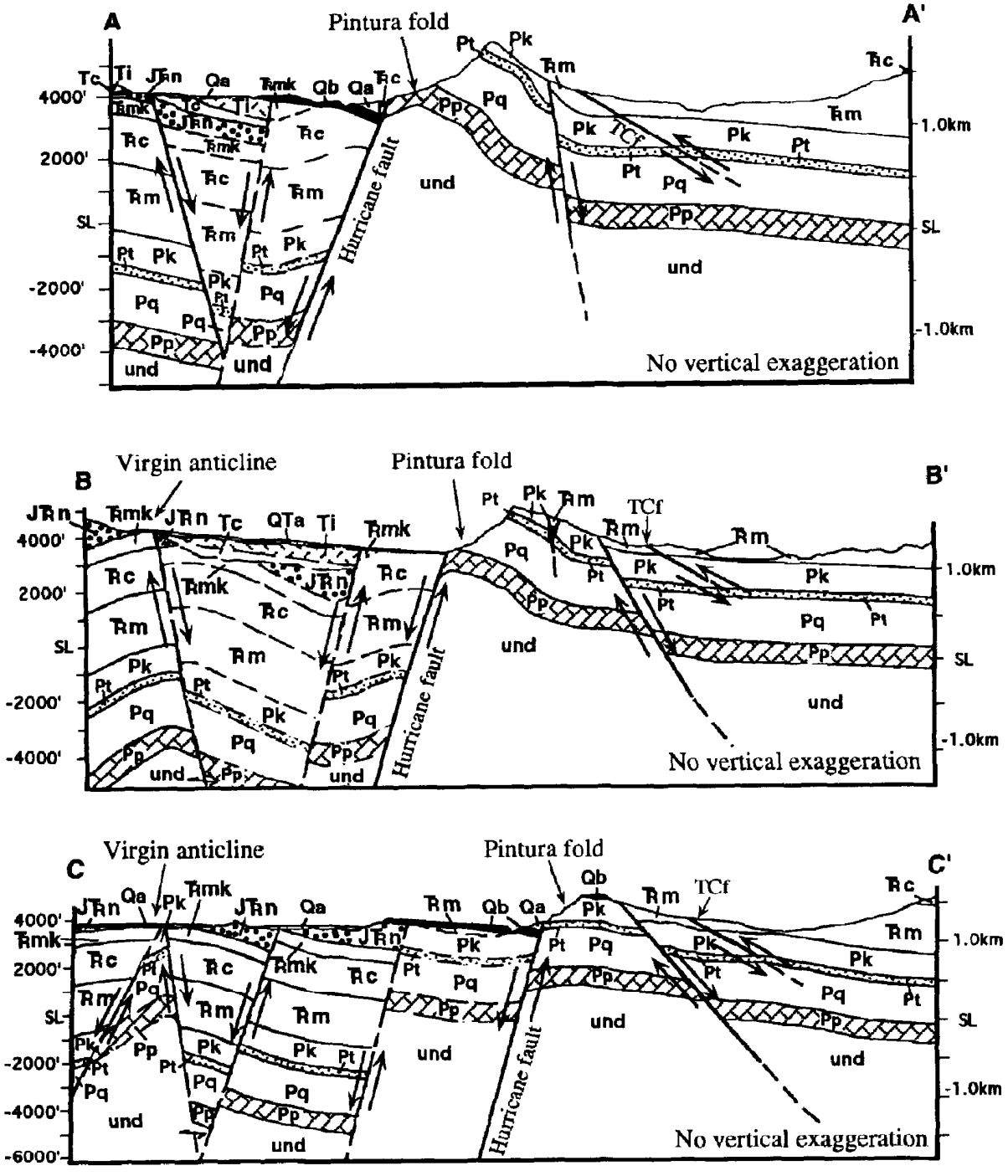

Fig. 4. Geologic cross-sections along A–A′ to D–D′ from Fig. 2. The Hurricane fault is labeled and, where appropriate, the Virgin Anticline and Pintura fold are marked. Faults are drawn with relative motion arrows; dashed fault lines indicate assumed faults. TCf = Taylor Creek.

The offset basalt sections are geochemically identical. Stratigraphic separation across the Hurricane fault prior to basalt extrusion ranges from 1740 m to 2070 m. Measurements are constrained by down-dropped outcrops of Triassic–Jurassic Navajo Sandstone in the hanging wall of the fault and projected locations based on stratigraphic thicknesses of the Navajo Sandstone in the footwall where it and the older units were eroded away. In the hanging wall, Quaternary basalt rests unconformably on Navajo Sandstone and in the footwall the geochemically identical basalt lies on Permian Kaibab Limestone. Total normal stratigraphic separation along the Hurricane fault is shown in cross-sections A–A′, B–B′ and C–C′ (Fig. 4). Assuming pure dip-slip as suggested above, along the A–A′ cross-section, line heave on the fault is 790 m and throw is 2130 m, and along the C–C′ line, the heave of the fault is 240 m and the throw is 1030 m. A local southward decrease in stratigraphic separation, heave and throw towards a major bend in the fault is suggested.

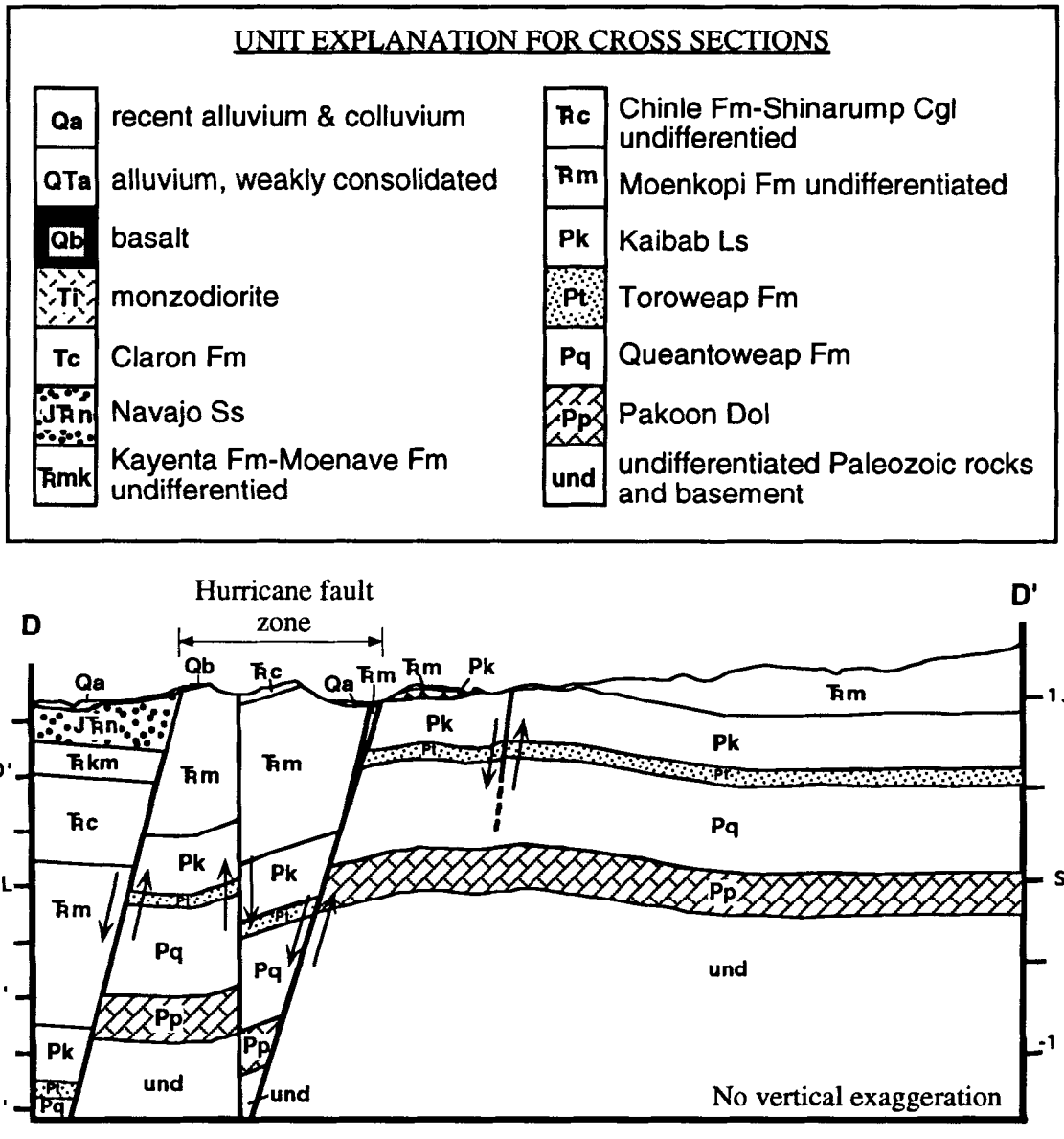

Fig. 4. (*Continued.*)

Fault sections

The Hurricane fault changes strike along its length (Fig. 2). In the south, the fault strikes N12°W (near '1' on Fig. 2). The fault is also a 1.5 km wide zone with several separate fault strands in this region (cross-section D–D' on Fig. 4). In contrast, the Hurricane fault is typically a single surface in the central and northern part of the study area (Fig. 2 and cross-sections A–A', B–B' and C–C' on Fig. 4). Northward, the fault strikes N37°W (near '2' on Fig. 2), and further north it strikes N13°W (near '3' on Fig. 2). The region of the fault with these three attitudes appears to form one fault segment that is generally concave towards the hanging wall with the southern area discussed here (near 1) near the center of the concave segment. Proceeding north (near '4' on Fig. 2), the strike changes to N21°E. Exposed fault surfaces along all sections dip approximately 70°W. The line of intersection between sections 3 and 4 plunges and trends 70°, N85°W and marks a major fault bend.

Late Quaternary fault activity

The Hurricane fault appears to be an active fault as indicated by: (1) offset Quaternary basalt; (2) offset Quaternary alluvium; and (3) recent seismic activity in the vicinity, such as the June 28–29, 1992, earthquake swarm (Arabasz *et al.* 1992a), the September 2, 1992, St. George earthquake (Arabasz *et al.* 1992b, Pechmann *et al.* 1992), as well as numerous small earthquakes that have occurred near the fault (Christenson & Nava 1992, S. J. Nava written communication 1993).

In three places along the Hurricane fault in the study area, unconsolidated Quaternary gravel or alluvium is offset. Two of the scarps are exposed in a displaced alluvial deposit, but the age of this deposit is unknown.

The largest fault scarp in the alluvium has a scarp slope of 30° and a scarp height of 6 m; another scarp has a slope of 15° and a 3 m height. Scarp slopes were measured from the angle made by the horizontal surface in the footwall of the scarp to the middle of the steep face of the scarp slope (Bucknam & Anderson 1979). At these two scarp sites, slip is apparently normal because alluvium is down-dropped in the hanging wall block. A third exposure of displaced Quaternary sediments is found in gravel in a narrow stream-cut channel where two fault strands crop out 3 m apart. This gravel is a basin deposit that accumulated in the depression adjacent to and formed by the Hurricane fault, but the age of the sediment is unknown. As much as 3 m of stratigraphic separation was measured along one strand that dips 60°W and 1.2 m of stratigraphic separation was measured along the other strand, a fault surface that dips 73°W and strikes N12°W. The present surface of the gravel is smooth; no typical fault scarp exists. Both the displaced alluvium and the basinal gravel deposit are older than the most recent sedimentation in the area. Exactly when fault motion created these scarps and offsets is unknown and it is not apparent whether motion was a single event or multiple events.

Pre-Quaternary fault activity

The discussion thus far has been confined predominantly to the utilization of data that formed during or after emplacement of the Quaternary basalt to address fault kinematics. This provides a relatively short period of observed motion along the Hurricane fault. It is obvious that the fault existed as a normal fault before the basalt was erupted because in the footwall, basalt flowed on to Permian rocks and in the hanging wall those same flow rocks lie on Triassic–Jurassic strata. No other clear kinematic indicators were found for the period before the lava flows, so the sense of motion on the Hurricane fault prior to basalt extrusion is not as simply defined as the Quaternary motion. The fault bend between sections 3 and 4 appears to have existed in roughly its present geometry prior to basalt extrusion because the basalt does not lap early fault strands. Additionally, no evidence was found for the Hurricane fault being a reactivated Sevier reverse fault as has been noted along other normal faults in the Basin and Range province and the transition zone (e.g. Royse *et al.* 1975, MacDonald 1976, Allmendinger *et al.* 1983, Villien & Kligfield 1986). Lastly, no exposures support or refute the theory of the Hurricane fault being a reactivated older structure, such as a Precambrian age fault (cf. Huntoon 1990).

Description of the regional folds

The Virgin anticline is a regional doubly plunging anticline (Fig. 1) exposed in Triassic–Jurassic Navajo Sandstone within the hanging wall of the Hurricane fault in the study area. In the field area, the anticline is upright, gently-plunging, open, and the fold axis orientation is 5°, S21°W (Figs. 2 and 4, cross-sections B–B′ and C–C′). Beds in the western limb of the Virgin anticline strike from N–S to N50°E and dip from 10° to 30° to the west. Bedding dips on the eastern limb of the anticline range from 10°E near the hinge to 41°E on the limb. The strike of beds on the eastern limb range from N12°E to N35°E.

The Pintura fold is an anticline exposed within the footwall of the Hurricane fault (Fig. 2) with a total along-strike length of approximately 23 km (Anderson & Mehnert 1979). The fold axis of the Pintura fold is oriented 8°S, 24°W and Permian rocks of the Pakoon, Queantoweap, and Toroweap Formations and Kaibab Limestone are exposed in the fold (Fig. 4, cross-sections A–A′, B–B′, and C–C′). Beds in the western limb of the Pintura fold strike from N10°E to N42°E and dips range from 14°W near the hinge to 75°W close to the Hurricane fault. The eastern limb of the fold contains beds that dip from 10° to 41° to the east and strike from N12°E to N35°E. The Pintura fold is an upright, gently-plunging to horizontal, open anticline. The shape of the fold may be distorted as a result of movement on the Hurricane fault; the effect of drag would be that beds in the western limb of the Pintura fold dip more steeply now than prior to faulting.

From Bouger gravity anomaly data gathered along the Hurricane fault (Cook & Hardman 1967), two apparent gravity highs occur on either side of the fault corresponding to the Virgin anticline and the Pintura fold. Between these two highs is a gravity low that is interpreted as a syncline. Hamblin (1965) mapped a syncline along strike to the south. A restoration of cross-section B–B′ shows both the Pintura fold and the Virgin anticline with a syncline between the two folds (Schramm 1994). These two anticlines and the syncline have similar wavelengths of about 10 km. The Virgin anticline and the syncline apparently parallel each other for at least 65 km along trend.

Both the Virgin anticline and the Pintura fold generally parallel regional structures related to Sevier compression (cf. Armstrong 1968). In the field area the Hurricane fault truncates the Pintura fold (Fig. 2). Further to the south, the Virgin anticline is cut by the Washington fault (Fig. 1), a regionally-related normal fault (Dobbin 1939, Hamblin 1970).

Small-scale contractional structures

A small displacement thrust fault is exposed in Permian Kaibab Limestone in the footwall of the Hurricane fault (Fig. 4, cross-section D–D′). This thrust has an attitude of approximately N56°W, 5°SW and a stratigraphic separation of up to 5 m. Although this thrust fault is cut by minor normal faults which have steep dips and strike between N10°W and N20°W, it occurs in a structurally complex area.

In the vicinity of the major bend between fault sections 3 and 4, a small-scale anticline is exposed in the hanging wall basalt (Fig. 2) with a 1°N, 72°E oriented hinge zone trending normal to the fault.

DISCUSSION

Interpreted slip direction

Using the vector information interpreted from the offset basalt, from N70°W to S18°W, the hanging wall dip data collected on basalt, the slickenline rakes and rake of the St. George earthquake, we suggest the direction of the vector of motion for the Hurricane fault to be about N75–85°W. If N75–85°W is the direction of motion along the entire fault length in this study area, then along the fault near site P, where the fault strikes N21°E, faulting is nearly pure dip-slip, and motion along the fault near sites AC and T, where the fault strikes N13°W, is also dip-slip but with a small dextral component. These data verify that in the Quaternary, no significant strike-slip motion occurred. In strike-slip scenarios, oblique en échelon folds may form in a narrow zone adjacent the fault in the hanging wall (Sylvester 1988) and none was observed. A N75–85°W vector agrees with stress field data based on earthquake focal mechanisms for the transition zone which indicates a S78°E–N78°W ±21° orientation (Zoback & Zoback 1980, Arabasz & Julander 1986).

Interpretation of fault segments and a segment boundary

Using the definition that a segmented fault has sections with unique strikes and/or shapes, the Hurricane fault is a segmented fault. Previously, no major fault segments nor segment boundaries were documented on the Hurricane fault, although Menges & Pearthree (1983) identified geometric changes in the Hurricane fault in Arizona. Identification of fault segments is critical because fault segment boundaries may be the sites of significant amounts of accumulated strain and may influence localization of earthquakes (Bruhn *et al.* 1990). Typically, a long (>200 km) normal slip fault such as the Hurricane fault will rupture along only some fraction of its length during a surface faulting event, and it is probable that segment boundaries control the location and extent of rupture (Schwartz & Coppersmith 1984). In this study, hanging wall and footwall shortening structures, scarp morphology, fault geometry, and increased complexity of faulting along the Hurricane fault are used to define a fault segment boundary and two fault segments along the Hurricane fault.

Where a fault surface is non-planar, some internal deformation in the hanging wall will occur (Scott *et al.* 1994). Along a segmented normal fault, anticlines that trend normal to the fault strike typically occur at or near fault segment boundaries (Schlische 1993). Fault segment boundary zones may be several kilometers wide (cf. Schwartz & Coppersmith 1984). The occurrence of a small-scale anticline in the basalt near the bend in the fault (Fig. 2) is strong evidence for a fault segment boundary there. The fault segment north of this anticline is here named the Ash Creek segment and south of the anticline the segment is here named the Anderson Junction segment (Fig. 2). A segment boundary at this location is also suggested by the large change in strike at the major bend in the fault; along the Anderson Junction segment the fault strikes N13°W near the segment boundary and along the Ash Creek segment the fault strikes N21°E.

Further evidence for a segment boundary is interpreted from the observation of less total stratigraphic separation along C–C′ than along A–A′ (Fig. 4). Cross-section C–C′ is at the segment boundary and A–A′ is constructed on the Ash Creek segment. This local decrease in displacement from the north to the bend in the fault would be expected if it has been a persistent barrier to slip (King 1986).

Antithetic and synthetic faults crop out along the Anderson Junction segment where the Hurricane fault is a zone as wide as 1.5 km (Fig. 4, cross-section D–D′). Antithetic faulting in the hanging wall occurs to fill space on a non-planar fault just as reverse drag fills space (Hamblin 1965, Gibbs 1984, Bruhn *et al.* 1987). A slight dextral component in slip on this fault segment might explain the complexity of faulting in this area as compared to other sections of the study area. This complexity might be caused by the slight pushing to the north of the hanging wall block and the consequent mismatch in the shapes of the hanging wall and footwall blocks. The fault bend between the Ash Creek segment and the Anderson Junction segment may essentially be a slight restraining bend where the hanging wall is moving towards the bend.

A restraining bend at the fault segment intersection requires creation of new faults and/or a change in the volume of rock. This restraining bend represents a non-conservative barrier whereby the multiple fault strands in the southern part of the field area accommodate slip along the fault that cannot be taken up solely on the main Hurricane fault. A non-conservative barrier occurs along segmented faults where the slip vector is not parallel to the line created by the intersection of fault segments, effectively creating space along the fault (cf. King 1986). The trend and plunge of the intersection line between the Ash Creek and Anderson Junction segments is approximately 70°N, 85°W, which roughly parallels the median vector of transport determined from dip analysis (N75°W) and lies within the range of vectors determined from offset basalt (73°N, 70°W to 75°S, 18°W) (cf. Janecke 1993, Evans & Langrock 1994). This approximate parallelism suggests a conservation of space across the fault plane, but field data suggest that there is, at least in part, some non-conservation of slip. The line of intersection between the fault segments does not exactly parallel the axial trend of the small-scale anticline in the footwall (1°N, 72°E), indicating the existence of a non-conservative barrier.

The small thrust fault in the footwall of the Hurricane fault near La Verkin Creek (Fig. 4, cross-section D–D′) may be related to extension. It is possible that, given the slight dextral component of motion on the fault in this vicinity, a northward push of the hanging wall block or local contraction of the footwall caused this thrust to form. The thrust's formation would be caused by

compression at a fault segment boundary. It is also possible, however, that the thrust fault is related to a smaller bend in the fault rather than the large strike change at the segment boundary; the fault strikes N12°W near '1' on Fig. 2 and further north, and north of the thrust, the strike of the fault is N37°W (near '2'). This again suggests that the thrust is related to extension with local compression at a fault bend.

On a segmented fault, unique segments will have unique rupture histories and offset in alluvium on each of the segments may indicate fault segment rupture history (Bruhn *et al.* 1987, dePolo *et al.* 1991, Machette *et al.* 1991, Zhang *et al.* 1991). Scarps in Quaternary alluvium are observed at two locations along the Ash Creek segment. Maximum scarp-slope angle versus scarp height data from the two scarps were plotted to determine a broad approximation of timing of faulting (Fig. 5). Over time a scarp degrades and its slope decreases (Nash 1980). The scarp-slope data points fall between the 1000 yr old Fish Springs scarp's regression line and the 15,000 yr old Bonneville shoreline scarp's regression line which were determined from previous scarp-slope studies in central Utah (Bucknam & Anderson 1979), suggesting that the timing of faulting along the Ash Creek segment can be approximated to between 1000 and 15,000 years ago. Clearly, scarp lay back angles are controlled by multiple variables (Pierce & Colman 1986). Such factors as alluvial cementation, slope aspect, vegetation, and microclimate were considered to be uniform on fault scarps in this study. Also, Bucknam & Anderson (1979) incorporated many scarp profiles into their study which allowed for smoothing of the data; we use this technique for general estimation of fault scarp timing purposes only.

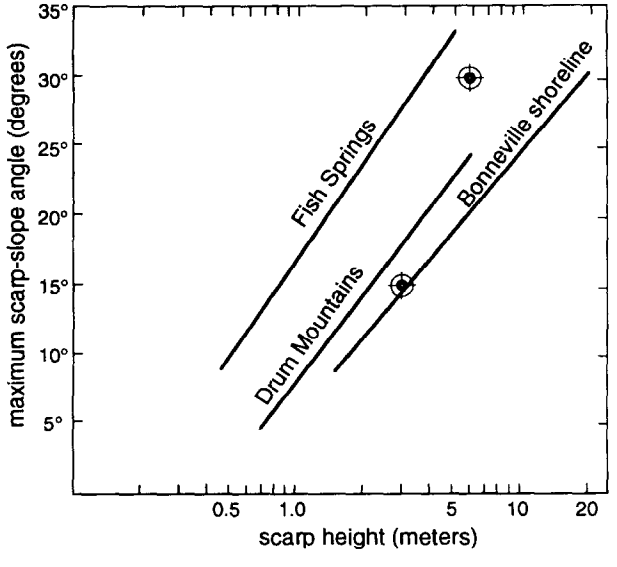

Fig. 5. Plot of maximum scarp-slope angle versus the scarp height for two scarps in the alluvium on the Hurricane fault in the field area (indicated by circle and cross symbols). The labeled regression lines are from scarp-slope data from the approximately 1000 yr old Fish Springs scarps, the 10,000 yr old Drum Mountains scarps, and the 15,000 yr old Bonneville shoreline scarps, all located in Utah, from Bucknam & Anderson (1979).

At one location along the Anderson Junction segment, offset in Quaternary gravel is exposed in a stream-cut channel. However the present surface of the gravel is relatively smooth; no scarp occurs here. The smaller amount of stratigraphic separation in the Quaternary sediment along the Anderson Junction segment than on the Ash Creek segment suggests that the two segments have differing faulting histories, which is expected along a segmented fault. Also, the lack of scarps along the Anderson Junction segment suggests the last surface rupture along it occurred before that of the Ash Creek segment.

The fault segments along the Hurricane fault can be further broken up into smaller fault sections. Within the field area the Anderson Junction segment comprises three fault sections, each with differing strikes (1, 2, and 3 of Fig. 2). Along strike the Anderson Junction segment is not continuously curved, but has discrete sections of nearly constant strike. The total length of the Anderson Junction segment may be at least, 19 km long or at most 45 km long, based largely on map view geometry and the major changes in the strike of the Hurricane fault (cf. Hintze 1980). However, a 45 km fault segment length for the Anderson Junction segment is longer than general maximum segment lengths (cf. Jackson & White 1989, dePolo *et al.* 1991). The Ash Creek segment may be 24 km long based on the same geometric criteria as above. A more detailed database of smaller scale mapping and trench studies along the Hurricane fault may help to better identify other major segments and boundaries.

Timing of hurricane fault motion and the relationship of the fault to nearby folds

The timing of first motion on the Hurricane fault is not well constrained by the available data. If it is assumed that the basalt in the field area is between 0.3 and 2 Ma and has been displaced 450 m, then it is possible considering the total stratigraphic separation of up to 2520 m to reasonably back calculate an age of initiation of faulting to the Pleistocene to Late Miocene. This, however, is highly conjectural and assumes a constant displacement rate.

Two large-scale anticlines, the Virgin anticline and the Pintura fold, crop out in the study area. The Pintura fold is truncated by the Hurricane fault and the Virgin anticline is cut by the Washington fault south of the study area. Based on these cross-cutting relationships, restoring the B–B′ cross-section (Fig. 4), and Bouger gravity evidence for the existence of a syncline paralleling and between the Virgin anticline and the Pintura fold (Cook & Hardman 1967), these folds are interpreted to be genetically related to each other and are older than extensional faults. Because the anticlines parallel nearby Sevier-age structures they are interpreted to be Sevier-related folds. Therefore, the Hurricane fault cuts across Sevier-age structures and is unlikely to be related to earlier thrust faults.

Duration of the geometric bend and segment boundary

Theories on fault growth suggest that geometric bends at fault segment boundaries typically form early in the history of the fault when (1) two (or more) propagating fractures approach each other and then link or (2) pre-existing fractures, such as joints, are linked by tensile fractures (Cowie & Scholz 1992a,b and references therein). We assume that the major bend in the Hurricane fault at the segment boundary formed early in the history of the fault as is consistent with existing fault growth theory and because no data, such as connecting older fault splays, were found to suggest that the fault has become curved or less planar with time. However, the geometry and kinematics of the hanging wall faults may indicate that the shape of the bend changed with time.

The large geometric bend between the Ash Creek and Anderson Junction segments is still present today and faulting histories across it are different. No major or mesoscale faults cut through the zone in the footwall at the bend which suggests that the fault has not broken through the segment boundary, although that may happen in the future (cf. Cowie & Scholz 1992b). Therefore, we suggest that in this case, and possibly in at least some other cases, the major geometric bends that formed at segment boundaries can last throughout much of the life of the fault. This suggestion does not require that the shape of the bend remain constant throughout that time. Although the time of initiation of movement on the Hurricane fault is not well known, movement most likely began during Late Miocene to Early Pliocene time. Thus, the bend between the Ash Creek and Anderson Junction segments appears to have been a major geometric element of the fault for a few to several million years. This time span is longer than has been previously suggested for the longevity of a segment boundary (Cowie & Scholz 1992b).

CONCLUSIONS

The Hurricane fault in southwestern Utah is an active, high-angle normal fault. Normal faulting formed up to 2070 m of stratigraphic separation prior to extrusion of Quaternary basalt. Following basaltic volcanism, there was an additional 450 m of stratigraphic separation for a total stratigraphic separation of 2520 m. Unconsolidated probable Quaternary gravels were displaced up to 6 m. From measurement of displaced geochemically identical basalt, slickenlines, an earthquake rake and basalt dip analysis, the relative motion for the northern portion of the fault in the field area, named the Ash Creek fault segment, is nearly perfect dip-slip. The relative motion in the southern section, the Anderson Junction segment, is dominantly dip-slip but has a slight dextral component to it.

The existence of a segment boundary between the Ash Creek and Anderson Junction fault segments is suggested by a small-scale anticline that crops out in Quaternary basalt in the hanging wall, a substantial change in fault strike in the same area, and changes in fault zone complexities. Also, a difference in timing of displacement on the segments is suggested by comparing the occurrence of two young scarps along the Ash Creek segment and the lack of a developed scarp along the Anderson Junction segment. The Anderson Junction segment has offset young sediments, but the surface has been beveled smooth. The two fault segments appear to have separate faulting histories and it can be expected that similar rupture events along these discrete segments will recur (cf. Schwartz & Coppersmith 1984, Bruhn *et al.* 1987, dePolo *et al.* 1991). The segment boundary is a non-conservative barrier and secondary faults in the hanging wall may be accommodating slip related to the fault (cf. King 1986). Right-normal motion along the Anderson Junction fault segment may have produced a small thrust fault in the footwall near a fault bend. The Anderson Junction segment has three fault sections within the field area (Fig. 2), although more may occur along strike. The Ash Creek segment may be 25 km long and the Anderson Junction segment is, at least, 19 km long.

We suggest that some geometric bends at fault segment boundaries can exist for a few to several million years, a time span longer than previously suggested. However, it is possible that the bends change shape over time. The geometric bend between the Ash Creek and Anderson Junction segments probably formed early in the history of the fault and persists today. Therefore, the geometric bend has existed for much of the life of the Hurricane fault which is probably at least 2 million years, but may be as much as 15 or 30 million years.

Acknowledgements—Financial support for this research was provided by grants from the Geological Society of America, Sigma Xi Grants-in-Aid, the University of Nevada, Las Vegas Graduate Student Association, the Business and Professional Women's Foundation Career Advancement program, the University of Nevada, Las Vegas Geoscience Department Scroungers Scholarship and the University of Nevada, Las Vegas–National Science Foundation Women in Science program (Cooperative Agreement OSR-9353227) to Stewart (formerly Schramm) and a University of Nevada, Las Vegas Grant and Fellowships Committee Research Grant to Taylor.

The manuscript was significantly improved by the careful editing of Gene Smith, Dave Weide, Michael Wells, Holly Langrock and Alex Sanchez and JSG reviewers Nancye Dawers, James Evans, and Philip Pearthree. The trace and major element analyses were performed by Shirley A. Morikawa at the University of Nevada, Las Vegas. Lehi Hintze, Gary Christenson, and Phil Pearthree offered helpful advice and support in the field.

REFERENCES

Allmendinger, R. W., Sharp, J. W., Von Tish, D., Serpa, L., Brown, L., Kaufman, S., Oliver, J. & Smith, R. 1983. Cenozoic and Mesozoic structure of the eastern Basin and Range province. Utah, from COCORP seismic-reflection data. *Geology* **11**, 532–536.

Anderson, R. E. & Barnhard, T. P. 1993. Heterogeneous Neogene strain and its bearing on horizontal extension and horizontal and vertical contraction at the margin of the extensional orogen, Mormon Mountains area, Nevada and Utah. *Bull. geol. Surv. U.S.A.* **2011**.

Anderson, R. E. & Christenson, G. E. 1989. Quaternary faults, folds and selected volcanic features in the Cedar City 1 × 2° quadrangle, Utah. *Utah Geol. Min. Surv. Misc. Pub.* **89-6**.

Anderson, R. E. & Mehnert, H. 1979. Reinterpretation of the history of the Hurricane fault in Utah. Rocky Mountain Association of

Geologists—Utah Geological Association, 1979 Basin and Range Symposium, 145–173.

Arabasz, W. J. & Smith, R. B. 1981. Earthquake prediction in the Intermountain seismic belt—An interplate extensional regime. In: *Earthquake Prediction—An International Review* (edited by Simpson, D. W. & Richards, P. G.). *Am. Geophys. Union, Ser.* **4**, 238–258.

Arabasz, W. J. & Julander, D. R. 1986. Geometry of seismically active faults and crustal deformation within the Basin and Range–Colorado Plateau transition of Utah. In: *Extensional Tectonics of the Southwestern United States—A Perspective on Processes and Kinematics* (edited by Mayer, L.). *Spec. Pap. geol. soc. Am.* **208**, 43–74.

Arabasz, W. J., Nava, S. J. & Pechmann, J. C. 1992a. Earthquakes near Cedar City, Utah, June 28–29, 1992. Univ. of Utah Seis. Stat. Preliminary Earthquake Rep.

Arabasz, W. J., Pechmann, J. C. & Nava, S. J. 1992b. The St. George (Washington County), Utah, earthquake of September 2, 1992. Univ. of Utah Seis. Stat. Preliminary Earthquake Rep.

Armstrong, R. L. 1963, K–Ar ages of volcanics in southwestern Utah and adjacent Nevada. In: *Guidebook to Geology of Southwestern Utah*. Intermtn. Assoc. petr. geol. Ann. Field Conf. Guidebook, 79–80.

Armstrong, R. L. 1968. Sevier orogenic belt in Nevada and Utah. *Bull. geol. Soc. Am.* **79**, 429–458.

Averitt, P. 1962. Geology and coal resources of the Cedar Mountain quadrangle, Iron County, Utah. *U.S. geol. Surv. Prof. Pap.* **389**.

Averitt, P. 1964. Table of post Cretaceous geologic events along the Hurricane fault near Cedar City, Iron County, Utah. *Bull. geol. Soc. Am.* **75**, 901–908.

Axen, G. J., Taylor, W. J. & Bartley, J. M. 1993. Space–time patterns and tectonic controls of Tertiary extension and magmatism in the Great Basin of the western United States. *Bull. geol. Soc. Am.* **105**, 56–76.

Best, M. G., McKee, E. H. & Damon, P. E. 1980. Space–time–composition patterns of late Cenozoic mafic volcanism, southwestern Utah and adjoining areas. *Am. J. Sci.* **280**, 1035–1050.

Best, M. G. & Grant, S. K. 1987. Stratigraphy of the volcanic Oligocene Needles Range Group in southwestern Utah. *U.S. geol. Surv. Prof. Pap.* **1433-A**, 3–28.

Best, M. G., Christiansen, E. H. & Blank, R. H. 1989. Oligocene caldera complex and calc–alkaline tuffs and lavas of the Indian Peak volcanic field, Nevada and Utah. *Bull. geol. Soc. Am.* **101**, 1076–1090.

Bruhn, R. L., Sibler, P. R. & Parry, W. T. 1987. Rupture characteristics of normal faults: an example from the Wasatch fault zone, Utah. In: *Continental Extensional Tectonics* (edited by Coward, M. P., Dewey, J. F. & Hancock, P. L.). *Spec. Publs. geol. Soc. Lond.* 337–353.

Bruhn, R. L., Yonkee, W. A. & Parry, W. T. 1990. Structural and fluid–chemical properties of seismogenic normal faults. *Tectonophysics* **175**, 139–157.

Bucknam, R. C. & Anderson, R. E. 1979. Estimation of fault-scarp ages from a scarp–height–slope–angle relationship. *Geology* **7**, 11–14.

Christenson, G. E. & Nava, S. J. 1992. Earthquake hazards of southwestern Utah. In: *Engineering and Environmental Geology of Southwestern Utah* (edited by Harty, K. M.). Utah Geol. Ass. Publ., 123–138.

Cook, E. F. 1952. Geology of the Pine Valley Mountains. A preliminary note. *Utah Geol. Min. Surv.* **7**, 92–100.

Cook, E. F. 1957. Geology of the Pine Valley Mountains, Utah. *Utah Geol. Min. Surv. Bull.* **58**.

Cook, K. L. & Hardman, E. 1967. Regional gravity survey of the Hurricane fault area and Iron Springs district. *Utah. Bull. geol. Soc. Am.* **78**, 1063–1076.

Cowie, P. A. & Scholz, C. H. 1992. Growth of faults by accumulation of seismic slip. *J. geophys. Res.* **97**, 11085–11095.

Cowie, P. A. & Scholz, C. H. 1992. Physical explanation for the displacement–length relationship of faults using a post-yield fracture mechanics model. *J. Struct. Geol.* **14**, 1133–1148.

Cowan, D. S. & Bruhn, R. L. 1992. Late Jurassic to Early Late Cretaceous geology of the U.S. Cordillera. In: *The Cordillera Orogen: Conterminous U.S.* (edited by Burchfiel, B. C., Lipman, P. W. & Zoback, M. L.). Geol. Soc. Am., DNAG, G3, 169–204.

dePolo, C. M., Clark, D. G., Slemmons, D. B. & Ramelli, A. R. 1991. Historical surface faulting in the Basin and Range province, western North America: Implications for fault segmentation. *J. Struct. Geol.* **13**, 123–136.

Dobbin, C. E. 1939. Geologic structure of St. George district Washington County, Utah. *Bull. Am. Ass. Petrol. Geol.* **23**, 121–144.

Evans, J. P. & Langrock, H. 1994. Structural analysis of the Brigham City–Weber Segment boundary zone, Wasatch normal fault, Utah: Implications for fault growth and structure. *Pure & Appl. Geophys.* **142**, 663–685.

Gardner, L. S. 1941. The Hurricane fault in southwestern Utah and northwestern Arizona. *Am. J. Sci.* **239**, 241–260.

Gibbs, A. D. 1984. Structural evolution of extensional basin margins. *J. geol. Soc. Lond.* **141**, 609–620.

Hamblin, W. K. 1965. Origin of 'reverse drag' on the downthrown side of normal faults. *Bull. geol. Soc. Am.* **76**, 1145–1164.

Hamblin, W. K. 1970. Structure of the western Grand Canyon region. In: *Guidebook to the Geology of Utah* (edited by Hamblin, W. K. & Best, M. G.). Utah Geol. Soc., 3–19.

Hintze, L. F. 1975. Geologic highway map of Utah. Brigham Young University Geol. Stud. Spec. Publ. 3, scale 1:1,000,000.

Hintze, L. F. 1980. Geologic map of Utah. Utah Geol. Min. Surv., scale 1:500,000.

Huntington, E. & Goldthwait, J. W. 1904. The Hurricane fault in the Toquerville district, Utah. *Harvard Coll. Mus. Comp. Zool. Bull.* **42**, 199–259.

Huntoon, P. W. 1990. Phanerozoic structural geology of the Grand Canyon. In: *Grand Canyon Geology* (edited by Beus, S. S. & Morales, S. M.). Oxford University Press, Museum of Northern Arizona Press, 261–309.

Hutchison, C. S. 1974. *Laboratory Handbook of Petrographic Techniques*. John Wiley and Sons, New York.

Jackson, J. A. & White, N. J. 1989. Normal faults in the upper continental crust: observations from regions of active extension. *J. Struct. Geol.* **11**, 15–36.

Janecke, S. U. 1993. Structures in segment boundary zones of the Lost River and Lemhi faults, east central Idaho. *J. geophys. Res.* **98**, 16223–16238.

King, G. C. P. 1986. Speculations on the geometry of the initiation and termination processes of earthquake rupture and its relation to morphology and geological structure. *Pure & Appl. Geophys.* **124**, 567–585.

Kurie, A. E. 1966. Recurrent structural disturbance of the Colorado Plateau margin near Zion National Park, Utah. *Bull. geol. Soc. Am.* **77**, 867–872.

Lay, T., Ammon, C. J., Velasco, A. V., Ritsema, J., Wallace, T. C. & Patton, H. J. 1994. Near-real time seismology: Rapid analysis of earthquake faulting. *GSA Today* **4**, 129–134.

Lovejoy, E. M. P. 1964. The Hurricane fault zone, and the Cedar Pocket Canyon–Shebit–Gunlock fault complex, southwestern Utah and northwestern Arizona. Unpublished Ph.D. dissertation, University of Arizona.

MacDonald, R. E. 1976. Tertiary tectonics and sedimentary rocks along the transition, Basin and Range Province to Plateau and Thrust Belt Province, Utah. In: *Symposium on Geology of the Cordilleran Hingeline* (edited by Hill, J. G.). Rocky Mountain Ass. Geol., 281–317.

Machette, M. N., Personius, S. F., Nelson, A. R., Schwartz, D. P. & Lund, W. R. 1991. The Wasatch fault zone, Utah—segmentation and history of Holocene earthquakes. *J. Struct. Geol.* **13**, 137–149.

Mackin, J. H. 1960. Structural significance of Tertiary volcanic rocks in southwestern Utah. *Am. J. Sci.* **258**, 81–131.

Menges, C. M. & Pearthree, P. A. 1983. Map of neotectonic (latest Pliocene–Quaternary) deformation in Arizona. *Arizona Bureau of Geol. Min. Tech. Open-file Rep.* **83-22**, 48.

Mills, J. G. 1991. The Timber Mountain Tuff, southwestern Nevada volcanic field: Geochemistry, mineralogy and petrogenesis. Unpublished Ph.D. dissertation, Michigan State University.

Moody, J. D. & Hill, M. J. 1956. Wrench-fault tectonics. *Bull. geol. Soc. Am.* **67**, 1207–1246.

Morikawa, S. A. 1993. The geology of the Tuff of Bridge Spring: Southern Nevada and northwestern Arizona. Unpublished Master Thesis, University of Nevada, Las Vegas.

Nash, D. B. 1980. Morphologic dating of degraded normal fault scarps. *J. Geol.* **88**, 353–360.

Nelson, S. T., Davidson, J. P. & Sullivan, K. R. 1992. New age determinations of central Colorado Plateau laccoliths, Utah: Recognizing disturbed K–Ar systematics and re-evaluating tectonomagmatic relationships. *Bull. geol. Soc. Am.* **104**, 1547–1560.

Noorish, K. & Hutton, J. T. 1969. An accurate X-ray spectrographic method for the analysis of a wide range of geological samples. *Geochim. Cosmochim. Acta* **33**, 431–453.

Pechmann, J. C., Arabasz, W. L. & Nava, S. J. 1992. The St. George, Utah, earthquake of September 2, 1992: A normal-faulting earthquake with very weak aftershock activity. *EOS (Trans. Am. geophys. Un.)* **73**, 399.

Pierce, K. L. & Colman, S. M. 1986. Effect of height and orientation (microclimate) on geomorphic degradation rates and processes, late-glacial terrace scarps in central Idaho. *Bull. geol. Soc. Am.* **97**, 869–885.

Reynolds, S. J. 1988. Geologic map of Arizona. Arizona Geol. Surv., scale 1:1,000,000.
Rowley, P. D., Steven, T. A., Anderson, J. J. & Cunningham, C. G. 1979. Cenozoic stratigraphic and structural framework of southwestern Utah. *U.S. geol. Surv.* **1149**.
Royse, F., Warner, M. A. & Reese, D. L. 1975. Thrust belt structural geometry and related stratigraphic problems, Wyoming–Idaho–northern Utah. In: *Symposium on Deep Drilling Frontiers in the Central Rocky Mountain.* Rocky Mountain Association of Geologists, 41–54.
Sanchez, A. 1995. Mafic volcanism in the Colorado Plateau/Basin-and-Range Transition Zone, Hurricane, Utah. Unpublished Master Thesis, University of Nevada, Las Vegas.
Schlische, R. W. 1993. Anatomy and evolution of the Triassic–Jurassic continental rift system, eastern North America. *Tectonics* **12**, 1026–1042.
Schramm, M. E. 1994. Structural analysis of the Hurricane fault in the transition zone between the Basin and Range province and the Colorado Plateau, Washington County, Utah. Unpublished Master Thesis, University of Nevada, Las Vegas.
Schwartz, D. P. & Coppersmith, K. J. 1984. Fault behavior and characteristic earthquakes: Examples from the Wasatch and San Andreas fault zones. *J. geophys. Res.* **89**, 5681–5698.
Scott, D. L., Braun, J. & Etheridge, M. A. 1994. Dip analysis as a tool for estimating regional kinematics in extensional terranes. *J. Struct. Geol.* **16**, 393–401.
Smith, R. B. & Sbar, M. L. 1974. Contemporary tectonics and seismicity of the western United States with emphasis on the Intermountain seismic belt. *Bull. geol. Soc. Am.* **85**, 1205–1218.
Susong, D. D., Janecke, S. U. & Bruhn, R. L. 1990. Structure of a fault segment boundary in the Lost River Fault Zone, Idaho, and possible effect on the 1983 Borah Peak earthquake rupture. *Bull. seism. Soc. Am.* **80**, 57–68.
Sylvester, A. G. 1988. Strike–slip faults. *Bull. geol. Soc. Am.* **100**, 1666–1703.
Taylor, W. J. & Bartley, J. M. 1992. Prevolcanic extensional breakaway fault and its geologic implications for eastern Nevada and western Utah. *Bull. geol. Soc. Am.* **104**, 255–266.
Villien, A. & Kligfield, R. M. 1986. Thrusting and synorogenic sedimentation in central Utah. In: *Paleotectonics and Sedimentation* (edited by Peterson, J. A.). *Mem. Am. Ass. Petrol. Geol.* **41**, 281–307.
Walker, J. D. 1986. The relation of tilt geometry to extension direction. *Geol. Soc. Am. Abs. with Programs* **18**(2), 194–195.
Watson, R. A. 1968. Structural development of the Toquerville–Pintura segment of the Hurricane Cliffs, Utah. *Brigham Young University Geol. Stud.* **15**, 67–76.
Zhang, P., Slemmons, D. B. & Mao, F. 1991. Geometric pattern, rupture termination and fault segmentation of the Dixie Valley–Pleasant Valley active normal fault system, Nevada, U.S.A. *J. Struct. Geol.* **13**, 165–176.
Zoback, M. L. & Zoback, M. D. 1980. State of stress in the conterminous United States. *J. geophys. Res.* **85**, 6113–6156.

APPENDIX

XRF laboratory methods

The following analytical methods are modified from Morikawa (1993). These are the standard methods employed at the University of Nevada, Las Vegas (UNLV).

Approximately 1–1.5 kg of fresh, unweathered sample was collected for each analysis. Samples were initially pulverized to <100 mesh in a Dyna Mill Supercollider air suspended impact attrition mill. A geochemical split (approximately 300 ml in volume) was separated from each pulverized sample and powdered to <200 mesh using a Pulverisette automated agate mortar and pestle.

Samples were processed into fused glass disks for major element analysis by heating 1.0 g sample, 9.0 g lithium tetraborate, and 0.16 g ammonium nitrate to 1100°C in gold–platinum crucibles and pouring the resultant melt into heated Au–Pt molds (Noorish & Hutton, 1969, Mills, 1991). Samples for trace element analysis were prepared by mixing a 2.5 g sample with 0.5 g methyl cellulose, enclosing this mixture with a rim and backing of additional methyl cellulose, and compressing to 10,000 psi in a Buehler specimen mount press to form a disk (Hutchison, 1974). All samples and reagents were weighted to ± 0.0002 g. All prepared samples were stored in desiccators prior to analysis.

XRF analyses were completed using the Rigaku 3030 XRF Spectrometer at UNLV.